energies

MDPI

*Article*

# Economic and Environmental Benefits for Electricity Grids from Spatiotemporal Optimization of Electric Vehicle Charging

**Soomin Woo [1], Zhe Fu [1], Elpiniki Apostolaki-Iosifidou [2,3,†] and Timothy E. Lipman [2,*]**

[1] Department of Civil and Environmental Engineering, University of California-Berkeley, Berkeley, CA 94720, USA; soomin.woo@berkeley.edu (S.W.); zhefu@berkeley.edu (Z.F.)
[2] Transportation Sustainability Research Center, University of California-Berkeley, Berkeley, CA 94704, USA; elpiniki.apostolaki@gmail.com
[3] Sustainability Solutions, ENGIE Impact, 1000 Brussels, Belgium
* Correspondence: telipman@berkeley.edu
† Apostolaki-Iosifidou was a postdoctoral researcher at the University of California, Berkeley, during this study.

**Abstract:** This article addresses the problem of estimating the potential economic and environmental gains for utility grids of shifting the electric-vehicle (EV) charging time and location. The current literature on shifting EV charging loads has been limited by real-world data availability and has typically therefore relied on simulated studies. Collaborating with a large automobile company and a major utility grid operator in California, this research used actual EV operational data and grid-operation data including locational marginal prices, marginal-grid-emission-rate data, and renewable-energy-generation ratio information. With assumptions about the future potential availability of EV charging stations, this research estimated the maximum potential gains in the economic and environmental performance of the electrical-grid operation by optimizing the time and location of EV charging. For the problem of rescheduling the charging sessions, the optimization models and objective functions were specifically designed based on the information available to the energy system operators that influence their economic and environmental performance like grid congestion, emissions, and renewable energy. The results present the maximum potential in reducing the operational costs and the marginal emissions and increasing the renewable energy use in the utility grid by rescheduling the EV charging load with respect to its time and location. The analysis showed that the objective functions of minimizing the marginal cost or the marginal emission rate performed the best overall.

**Keywords:** electric vehicle; charge management; smart charging; vehicle grid integration; load shifting; marginal emissions; renewable energy



**Citation:** Woo, S.; Fu, Z.; Apostolaki-Iosifidou, E.; Lipman, T.E. Economic and Environmental Benefits for Electricity Grids from Spatiotemporal Optimization of Electric Vehicle Charging. *Energies* **2021**, *14*, 8204. https://doi.org/10.3390/en14248204

Academic Editor: Branislav Hredzak

Received: 29 October 2021
Accepted: 30 November 2021
Published: 7 December 2021



## 1. Introduction

Electric vehicles (EVs) are now proliferating in major automobile markets around the world. Despite the environmental benefits of EVs for air quality, greenhouse-gas emissions, and human health [1], EVs can add significant electrical loads and cause potential negative impacts for electrical-grid operations, such as grid congestion, violations of voltage limits, and heavy loading of network assets (e.g., distribution transformers) [2,3]. EV load is not characterized only by the time of the day that takes place but also by geographical location and the specific section of the distribution grid where the load is connected. Therefore, EV charging solutions that are based on both time and location can be important to potentially reducing the impacts of EVs on the grid. Managing the timing and location of EV charging is becoming increasingly possible as the battery capacity of EVs grows larger, and also because personal vehicles including EVs spend most of the time parked and have large time windows in which to charge.

In this study, we addressed the problem of estimating the maximum potential gains in terms of economics, the integration of renewable energy sources, and greenhouse-

gas emission reductions for electrical-grid operators in shifting the time and location of charging EVs based on a real-world study. For background, there is a large body of research that optimizes EV charging to improve the performance of electrical-grid operation. Optimal charging schedules for EVs can improve various aspects of grid operations, such as reducing costs, emissions, peak loads, power losses, and integration of renewable energy sources [4,5]. However, there can be trade-offs between improving one aspect at the expense of another. For instance, EV-charging schedules that target nighttime charging to reduce electricity costs can result in higher emissions of carbon dioxide [6]. Additionally, attempts to optimize overnight EV charging with respect to a time-of-use pricing regime can increase the curtailment of renewable energy [7]. In the current literature, it is not clearly identified which performance metric of the grid operation one must target in optimizing the EV charging so that the grid performance improves holistically without foregoing another.

In addition, some studies use performance metrics that are not easily measurable or directly useful on the grid operators. For instance, Kara et al. [8] optimized EV charging by shaving the peak demand; Tarroja et al. [9] shifted the charging load to hours with high renewable generation; and Jian et al. [10] filled the valley and shaved the peak of the energy demand. However, managing EV charging with these objectives may not lead directly to cost reduction, emission reduction, or an increase in renewable energy use. These performance metrics will be easier to use in practice if the values are easily measurable and immediately useful to the grid operator.

Additionally, most of the literature has been limited in studying optimal charging at fixed locations, i.e., changing the charging time or charging power within each plug-in session to improve the operation of the electrical grid [5,7–13]. However, there is a significant benefit to relocating charging sessions as well, for example, from the home to the workplace so that EVs charge midday and use solar energy [14]. Szinai et al. [7] also found that there is only little value in smart charging at fixed locations at workplaces because people often charge at home. Therefore, we investigated the benefit of optimal EV charging by not only shifting the time of charging within each plug-in session but also choosing the charging location across the places that the vehicle visits. Expanding the solution space of charging decisions in both time and space allowed us to enhance the benefits in optimal charging.

With EV-charging control, many studies attempt to estimate potential improvements to electrical-grid operation. However, most studies depend only on aggregated or simulated data on the driving and charging demand of EVs because real data for individual EVs are scarce. Examples of studies that use aggregate data include the work by Kara et al. [8], which uses the aggregate charging demand of the EVs and the "load flexibility" of EVs, i.e., the ratio of charging time to the parking time, to estimate the maximum benefit in shaving the demand peak. Similarly, Teng et al. [11] used an aggregate EV-charging demand and aggregate flexibility to estimate the reduction in grid operation cost, though the demand and flexibility values were calculated from individual EVs and their mobility constraints.

Examples of studies that simulate the driving and charging of EVs based on the United States National Household Travel Survey include the work by Tarroja et al. [9], which calculated the reduction in emissions and fuel for the vehicles on the road and estimated the increase in renewable energy use. Forrest et al. [12] used the survey data to simulate EVs and estimate the economic and environmental value of renewable-energy integration. Van Triel and Lipman [5] simulated EVs and grid operation based on the survey data and calculated the reduction in renewable energy curtailment and consequently avoided installment of the energy storage system. Other interesting examples of simulation studies include Jian et al. [10], who simulated the charging load of millions of EVs and estimated the peak energy demand with EV charging management. Szinai et al. [7] simulated the detailed travel and charging demand of EVs with an agent-based model called BEAM and a grid-operation model called PLEXOS and estimated the maximum benefit in reducing the cost and the renewable energy curtailment with EV-charging management.

In this article, we present an analysis based on the actual driving and charging behavior of hundreds of EVs operating in the San Francisco Bay Area in California. We collaborated with an automobile company (BMW North America LLC, Woodcliff Lake, NJ, USA), a grid operator (Pacific Gas and Electric Company or PG&E, San Francisco, CA, USA), a grid-services company (Olivine Inc., Berkeley, CA, USA), and an energy data-analytics company (Kevala Analytics, San Francisco, CA, USA). We combined grid data for corresponding locations and times, along with the real-world data for driving and charging individual EVs. With this rich set of data, we estimated the electrical grid benefit from optimal charging as realistically as possible. The grid data included the locational marginal price (LMP), the marginal-emission rate (MER), and the renewable-energy (RE) ratio, which were measurable to grid operators. The data used in the analysis are explained in more detail in Section 3.

Our contribution to the current knowledge in EV charging and its benefit to the electrical-grid operation is threefold. First, we identified and recommended an objective function to optimize EV-charging sessions so that the grid operation can improve holistically in terms of operation costs, greenhouse-gas emissions, and renewable energy integration. These objective functions were developed based on measurable and immediately useful values to the grid operator. Second, we developed an algorithm that optimizes both the time and location of charging individual EVs to enhance electrical-grid operation. With assumptions on charging compliance, data availability, and perfect knowledge, we estimated the maximum benefit that the algorithm can bring in reducing the operation cost, reducing the greenhouse gas emissions, and increasing the renewable energy usage. Third, we overcame the limitations in simulating and aggregating the behavior of EVs by using the real driving and charging data of individual EVs and grid-operation data in California. This allowed us to realistically estimate the benefit of optimal charging to the grid operation.

Our research is presented as follows. In Section 2, we describe three performance metrics of electrical-grid operation based on the LMP, the MER, and the RE ratio, for which EV charging was optimized. We propose two optimization models: (1) a fixed-Location model to schedule only the time to charge EVs and (2) an inter-location model to schedule both the time and location to charge EVs. These two models can solve objective functions for the three performance metrics. We also describe how we evaluated the performance of the optimization models. In Section 3, we describe the real data from California used in this research, namely, the telematics data of individual EVs on driving and charging and the operational data for the local electrical grid. We also briefly explain how the data were processed for this research. In Section 4, we verify the fixed-location model and the inter-location model with sample trajectories of charging power for individual vehicles and validate the model performance in terms of the electrical-grid operation for charging a fleet of EVs. We estimate the maximum gain to electrical-grid operation from controlling EV charging time and location, in terms of cost savings, emission reductions, and renewable-energy usage. Finally, we compare the performance of six cases (two optimization models and three objective functions) and recommend a policy that can reduce grid operation cost and greenhouse gas emissions and increase the usage of renewable energy. The article is concluded in Section 6.

## 2. Methodology

We proposed two optimization models to schedule the charging time and location of EVs and explain how we evaluate the performance of optimization models in generating benefits to the electricity-system operator. We first describe three metrics, namely, the locational marginal price (LMP), the emission rate, and the renewable-energy ratio, to reflect the economic and environmental performance of the local electrical grid. We used these metrics to develop the objective functions and proposed two optimization models to solve them. These are the fixed-location model and the inter-location model. We then describe

the methodology to conduct a case study of real EV drivers in California to evaluate the potential benefits to the system operator in optimizing the EV charging schedule.

### *2.1. Performance Metrics of Electrical Grid*

We choose the LMP, the MER, and the RE percentage to evaluate grid performance because they are measurable values by the grid operator. We used the LMPs as defined by the transmission system operator of California, the California Independent System Operator (CAISO). LMP is the marginal cost of delivering the energy in units USD per MWh, commonly understood as the wholesale electricity cost, and it is used to control electricity grid congestion and to optimize power flow [15]. CAISO sets LMPs at nodes, including scheduling points, and aggregated pricing nodes. The distance between the nodes can be from less than a mile to several miles. The LMP value changes for each node and each time interval and shows inter-location variations based on the marginal cost of energy, power losses, and grid congestion. In this study, the LMP metric was used independently of the distribution grid and its components (distribution transformers). An example of an hourly LMP trend at a node is shown in Figure 1. The figure shows that there is a sharp increase in pricing in the morning before work hours and in the afternoon when people return home. We defined a parameter for LMP, $C_{\mathrm{LMP}}(t, x)$, as the locational marginal price at time $t$ and node $x$, converted to USD per kWh.

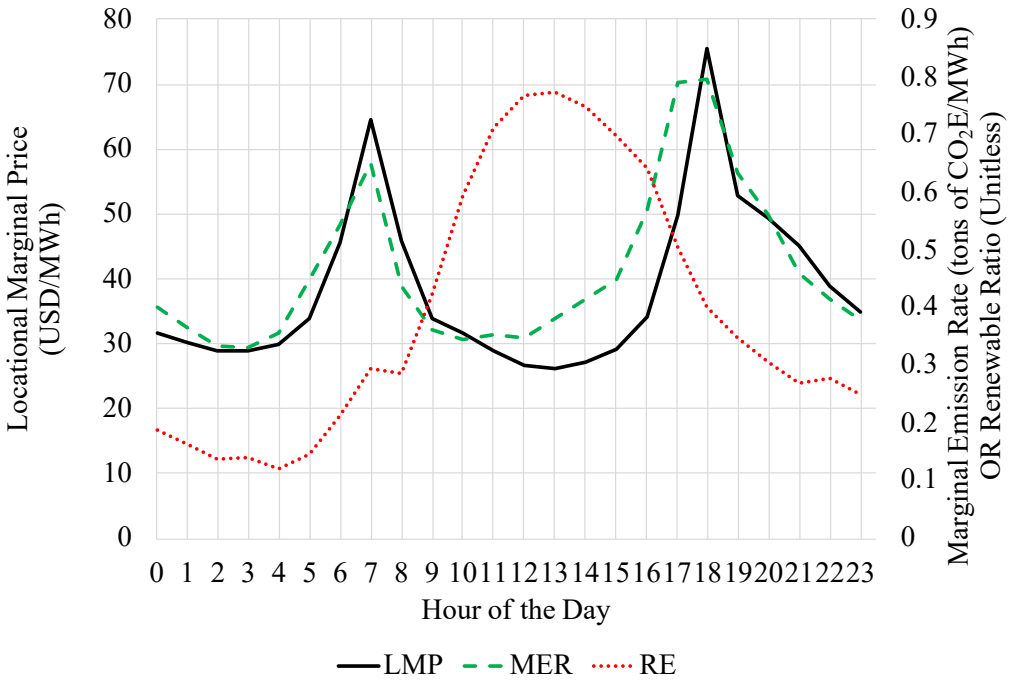


**Figure 1.** Example of locational marginal pricing, the marginal-emission rate, and the renewable ratio (2 November 2017, LMP node ID: BAYSHOR2-1-N001, SubLAP: PGSF).

For the emission rate, we used the MER of greenhouse gases in California. The MER is the rate of emissions that are produced when additional load is added and new generation subsequently comes online. The MER is expressed as the marginal emissions in units of tons of $CO_2E$/MWh. This greenhouse-gas-intensity metric was extracted from the 2019 avoided-cost calculator (ACC) model, developed by E3 consulting. Figure 1 shows an example of the MER values; these change over time and location. However, we assumed these were independent of the location due to the data availability. Similar to the trend of LMP, there are two peaks: one in the morning and another in the afternoon. We defined $C_{\mathrm{MER}}(t)$ as the marginal emission rate at time $t$, converted to tons of $CO_2E$/kWh.

As for the renewable energy (RE) ratio, we used the data provided by PG&E indicating the unitless ratio of the generated RE. This provides the RE ratio for each hour that does not

change with location within the PG&E service territory. An example of the hourly RE ratio is shown in Figure 1. The RE ratio has a different trend from LMP and MER, with one peak that appears around noon through early afternoon when solar energy is largely generated. The RE ratio is low during the evening and before sunrise. We defined $C_{\mathrm{RE}}(t)$ as the RE ratio at time $t$, without units.

Note that in the following formulation of the optimization models, we assumed the knowledge of values for $C_{\mathrm{LMP}}(t,x)$, $C_{\mathrm{MER}}(t)$, and $C_{\mathrm{RE}}(t)$ at all times and locations, where vehicles are present over the optimization time window.

### *2.2. Optimization Models*

In this section, we first describe the vehicle, time, and location notation. We proposed the fixed-location model and the inter-location model to schedule the charging of individual EVs, as well as the three objective functions for each model. We also explain the evaluation method of the proposed models.

#### 2.2.1. Notation

We defined vehicle index $i \in [1, N_{EV}]$, where $N_{EV}$ is the sample size of EVs. We defined the destination index that vehicle $i$ visits as $k \in [1, K_i]$ over the optimization time horizon. For each vehicle $i$, its battery capacity in energy was assumed as $E_{b,i}$. For each destination $k$, a tuple of parameters are known: $(T^a_{i,k}, T^d_{i,k}, E^{des}_{i,k}, E^c_{i,k})$, which are the arrival time to the node, the departure time from the node, the desired charging energy at the node, and the energy consumption for the trip departing from the node, respectively. These notations are shown in Figure 2 with arrivals and departures of a vehicle $i$ over time $t$. Note that the energy consumption to the first location in the sample was disregarded, and the initial energy level $E_{ini,i}$ was evaluated at the arrival of the first location. Note that we assumed the parameter tuples shown in the graph to be known. If there was no information of final departure, we assumed that its time coincided with the final arrival and that the final desired charging energy was zero.

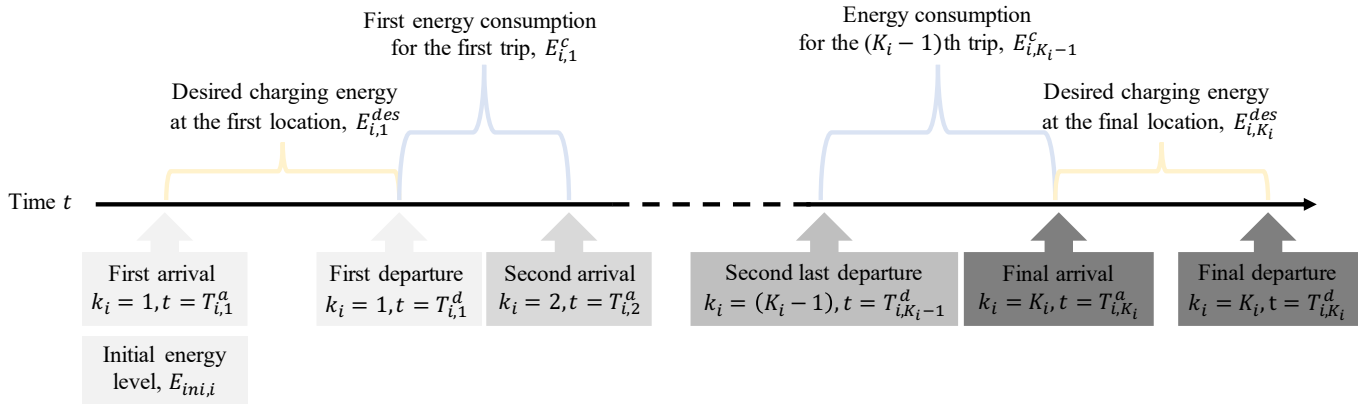


Nomenclature

- $i \in [1, N_{EV}]$: vehicle index, where $N_{EV}$ is the sample size of EVs
- $k_i \in [1, K_i]$: destination index of $i$-th vehicle, where $K_i$ is the total number of destinations of the vehicle
- $T^a_{i,k}, T^d_{i,k}$: $i$-th vehicle's arrival time to the $k$-th destination and departure time from the $k$-th destination, respectively
- $E_{ini,i}$: $i$-th vehicle's initial energy level
- $E^{des}_{i,k}$: $i$-th vehicle's desired charging energy at the $k$-th destination
- $E^c_{i,k}$: $i$-th vehicle's energy consumption in the trip from the $k$-th destination

**Figure 2.** Notations to describe the multiple destinations for a vehicle.

In addition, we defined a binary parameter to indicate the known information on the parking status as $S_i(t)$, which equals 1 if the vehicle $i$ is parked at time $t$ and 0 otherwise.

Additionally, for each time step $t$, the electrical grid node that the vehicle's location belongs to is expressed as $\hat{x}_i(t)$. We assumed that only $S_i(t) \cdot \hat{x}_i(t)$ is known; in other words, we know the grid node that the vehicle is connected to, only if it is parked.

2.2.2. Fixed-Location Charging Optimization

The fixed-location model schedules the charging time of an individual EV at a given location, by exploiting the variation in the LMP, the MER, and the RE ratio over time. The model assumes that the EV can charge at various power levels under its physical capacity once it is plugged in. The EV may not start to charge immediately upon plugging in, but it can also defer its charging during the plugging session. The model requires the provision of the demanded energy at each destination. The model was applied for all destinations of all EVs in the sample, and the total gains in the LMP, the MER, and the RE were computed for the aggregate EVs.

Three optimization problems are given below. We minimized the LMP cost in units of USD as shown in (1a), minimized the MER metric in units of tons of $CO_2E$ as shown in (1b), and maximized the RE in units of MWh as shown in (1c). The optimization variable was the charging power at each time step, $P_c(i,t)$ for vehicle $i$ in units of kW. The optimization time $t$ ranged over $[T^a_{i,k}, T^d_{i,k}]$ with a discrete interval of $\Delta t = 1$ h.

$$\min_{P_c(i,t)} \; J_{\mathrm{LMP,i,k}},$$

$$J_{\mathrm{LMP,i,k}} = \Delta t \sum_{t=T^a_{i,k}}^{T^d_{i,k}} P_c(i,t) \cdot C_{\mathrm{LMP}}(t, \hat{x}_i(t)) \tag{1a}$$

$$\min_{P_c(i,t)} \; J_{\mathrm{MER,i,k}},$$

$$J_{\mathrm{MER,i,k}} = \Delta t \sum_{t=T^a_{i,k}}^{T^d_{i,k}} P_c(i,t) \cdot C_{\mathrm{MER}}(t) \tag{1b}$$

$$\max_{P_c(i,t)} \; J_{\mathrm{RE,i,k}},$$

$$J_{\mathrm{RE,i,k}} = \Delta t \sum_{t=T^a_{i,k}}^{T^d_{i,k}} P_c(i,t) \cdot C_{\mathrm{RE}}(t) \tag{1c}$$

To constrain the physical-charging capacity of vehicles, we constrained the charging power, $P_c(i,t)$ by the rated charging power of the vehicle $i$, $P_{r,i}$. We also modeled the desired charging energy, $E^{des}_{i,k}$, during the stay at location $k$. The constraints for the fixed-location optimization are given below:

$$0 \le P_c(i,t) \le P_{r,i} \tag{2}$$

$$E^{des}_{i,k} \le \Delta t \sum_{t=T^a_{i,k}}^{T^d_{i,k}} P_c(i,t) \tag{3}$$

As a simplification, we assumed there was negligible energy loss in charging. Since the optimization problem is linear and convex, the optimization result is globally optimal. We used the constraints (2) and (3) to solve three optimization problems in terms of the LMP, the MER, and the RE, by choosing (1a), (1b), or (1c), respectively. We applied

this optimization problem to each parking instance of individual EVs in an optimization horizon. The performance of the fixed-location model can be expressed as the following:

$$\widehat{J_{\text{agg, LMP}}} = \sum_{i=1}^{N_{\text{EV}}} \sum_{k=1}^{K_i} J_{\text{LMP,i,k}} \left( \underset{P_c(i,t)}{\text{argmin}}\, J_{\text{LMP, i,k}} \right) \tag{4a}$$

$$\widehat{J_{\text{agg, MER}}} = \sum_{i=1}^{N_{\text{EV}}} \sum_{k=1}^{K_i} J_{\text{MER,i,k}} \left( \underset{P_c(i,t)}{\text{argmin}}\, J_{\text{MER, i,k}} \right) \tag{4b}$$

$$\widehat{J_{\text{agg, RE}}} = \sum_{i=1}^{N_{\text{EV}}} \sum_{k=1}^{K_i} J_{\text{RE,i,k}} \left( \underset{P_c(i,t)}{\text{argmax}}\, J_{\text{RE, i,k}} \right) \tag{4c}$$

where (4a), (4b), and (4c) evaluated the total minimized LMP cost, the total minimized MER, and the total maximized RE ratio, respectively, on aggregate EVs over a given optimization horizon. We assumed that the change in charging schedule in individual EVs does not affect the LMP, the MER, and the RE.

2.2.3. Inter-Location Charging Optimization

The inter-location model expands the feasible solution set from the fixed-location model by scheduling not only when to charge but also where to charge among the locations that the EV parks. This model assumes that, in the future, every destination that an EV visits has a charger available to use. The inter-location model exploits the LMP, MER, and RE values that vary over time across multiple locations that the vehicle visits. This model finds the optimal time and location to charge, while satisfying the energy needs to drive between the locations, a minimum and maximum energy level for each vehicle, and a final condition for the battery state-of-charge level at the end of the optimization horizon. The model was applied for all EVs in the sample and the total gains in the LMP, the MER, and the RE were computed for the aggregate EVs.

Three objective functions were proposed. We minimized the LMP cost in USD as shown in (5a), minimized the greenhouse-gas emissions in unit of tons of $CO_2E$ as shown in (5b), and maximized the RE ratio of energy generation provided to charge the vehicle as shown in (5c).

$$\begin{aligned} &\min_{P_c(i,t)} \; J_{\text{LMP,i}}, \\ &\qquad J_{\text{LMP,i}} = \Delta t \sum_{t=T_{i,1}^a}^{T_{i,K_i}^d} P_c(i,t) \cdot C_{\text{LMP}}(t, \hat{x}_i(t)) \end{aligned} \tag{5a}$$

$$\begin{aligned} &\min_{P_c(i,t)} \; J_{\text{MER,i}}, \\ &\qquad J_{\text{MER,i}} = \Delta t \sum_{t=T_{i,1}^a}^{T_{i,K_i}^d} P_c(i,t) \cdot C_{\text{MER}}(t) \end{aligned} \tag{5b}$$

$$\begin{aligned} &\max_{P_c(i,t)} \; J_{\text{RE,i}}, \\ &\qquad J_{\text{RE,i}} = \Delta t \sum_{t=T_{i,1}^a}^{T_{i,K_i}^d} P_c(i,t) \cdot C_{\text{RE}}(t) \end{aligned} \tag{5c}$$

The optimization problems in (5a), (5b) and (5c) are similar to those in (1a), (1b), and (1c); however, they are different in the optimization time range. The inter-location problem spans multiple locations that each vehicle visits, i.e., for vehicle $i$, the optimization searches a solution from the arrival time at the first location, $T_{i,1}^a$ until the departure time of

the final (or $K_i$-th) location, $T^d_{i,K_i}$. The optimization variable is the charging power at each time step $t$ for vehicle $i$, $P_c(i,t)$.

The inter-location model limits the charging power by the rated charging power, $P_{r,i}$, and also by its parking status $S_i(t)$. Refer to (6) below where the charging power is forced to be zero when the vehicle is on the move, i.e., $S_i(t) = 0$.

$$0 \leq P_c(i,t) \leq S_i(t) \cdot P_{r,i} \tag{6}$$

The model also develops a schedule to satisfy the necessary energy for the trips and to maintain the energy level of EV to belong within a given range, $(E_{min,i}, E_{max,i})$. We assumed $E_{min,i} = 0.10 \cdot E_{b,i}$ and $E_{max,i} = E_{b,i}$, respectively. At arrival to each destination after the first destination, we checked that the vehicle's initial energy level $E_{ini,i}$ and the cumulative charging energy satisfied the cumulative energy consumption as shown in (7). For all $q = 2, ..., K_i - 1$,

$$E_{min,i} \leq E_{ini,i} + \Delta t \sum_{t=T^a_{i,1}}^{T^a_{i,q}} P_c(i,t) - \sum_{p=1}^{q-1} E^c_{i,p} \leq E_{max,i} \tag{7}$$

This constraint provides a minimum energy to the vehicle for the duration of the upcoming trip. For instance, at arrival to the second destination ($q = 2$), the sum of the initial energy level, the cumulative charging energy at the first location, and the energy consumption to the second location must be within the range, $(E_{min,i}, E_{max,i})$.

The energy level was also checked at all departures; refer to (8). For all $q = 1, ..., K_i - 1$,

$$E_{min,i} \leq E_{ini,i} + \Delta t \sum_{t=T^a_{i,1}}^{T^d_{i,q}} P_c(i,t) - \sum_{p=1}^{q-1} E^c_{i,p} \leq E_{max,i} \tag{8}$$

This constraint prevents the vehicle from charging over its battery capacity. For instance, at departure from the first destination ($q = 1$), the sum of the initial energy level and the cumulative charging energy at the first destination must be in the range $(E_{min,i}, E_{max,i})$ as $E^c_{i,0} = 0, \forall i$. At departure from the second destination ($q = 2$), the sum of the initial energy level, the cumulative charging energy, and the cumulative energy consumption to the second location must be in the range $(E_{min,i}, E_{max,i})$.

We also enforced a final condition for the battery energy level to be at least 50%, i.e., $E_f = 0.50 \cdot E_{b,i}$, to prevent the solution from depleting the EV energy by the final time step, as below:

$$E_{ini,i} + \Delta t \sum_{t=T^a_{i,k}}^{T^d_{i,K_i}} P_c(i,t) - \sum_{k=1}^{K_i} E^c_{i,k} \leq E_f \tag{9}$$

Here again, we assumed there is negligible energy loss in charging. Since the optimization problem is linear and convex, the optimization result is globally optimal. We used the constraints (6)–(9) to solve three optimization problems in terms of the LMP, the MER, and the RE by choosing (5a), (5b), or (5c), respectively. We applied these optimization problems to each individual EV over a time period, such as one month. In other words, we optimized from the arrival time at the first destination to the departure time from the last

destination within a month for each vehicle. The performance of the inter-location model can be expressed as the following:

$$\widehat{J_{\text{agg, LMP}}} = \sum_{i=1}^{N_{\text{EV}}} J_{\text{LMP, i}}\left(\underset{P_c(i,t)}{\text{argmin}}\, J_{\text{LMP, i}}\right) \tag{10a}$$

$$\widehat{J_{\text{agg, MER}}} = \sum_{i=1}^{N_{\text{EV}}} J_{\text{MER, i}}\left(\underset{P_c(i,t)}{\text{argmin}}\, J_{\text{MER, i}}\right) \tag{10b}$$

$$\widehat{J_{\text{agg, RE}}} = \sum_{i=1}^{N_{\text{EV}}} J_{\text{RE, i}}\left(\underset{P_c(i,t)}{\text{argmax}}\, J_{\text{RE, i}}\right) \tag{10c}$$

where (10a), (10b), and (10c) evaluate the total minimized LMP cost, the total minimized MER, and the total maximized RE ratio, respectively, on aggregate EVs. We assumed that the change in charging schedule in individual EVs did not affect the values of the LMP, the MER, and the RE.

### *2.3. Performance Evaluation*

We thus proposed two optimization models and three objective functions to solve for each model. We first present the detailed results of each model in minimizing the LMP cost, i.e., solving (1a) and (5a). We validated each model with the sample trajectories of charging power for an individual vehicle. We evaluated the performance of both models by analyzing the EV sample size (veh), the total parking hours (veh-hr), the total charging hours (veh-hr), the total hours with change in charging status (hrs), the total change in the LMP cost (USD), and the average change in the LMP cost (USD/veh-hr).

The total parking (or charging) hours were computed as the sum of parking (or charging) hours of all vehicles in the sample. We used the term "idle" to describe the charging status of vehicle that is parked but not charging. The total hours with the change in charging status calculates the sum of hours such that the vehicle's charging status is different in the optimization result from the actual data. For instance, there is a 1-h change in status if a vehicle was charging from 8:00 a.m. to 8:30 a.m. (or up to 9:00 a.m.) in the actual data, but the optimization result recommends it to be "idle". The total change in theLMP cost is the optimized LMP cost (the values of (4a) or (10a)), subtracted by the total LMP cost in actual data. The total change in the LMP cost is negative when LMP costs are saved with optimization. The average change in the LMP cost is the total change in the LMP cost, divided by the total parking hours in the actual data.

Additional analysis was performed for the inter-location model results by grouping them based on various destinations. These included anonymized home locations, "away" locations (destinations other than the home locations), and two regional units called sub-load aggregation Points (SubLAPs). The SubLAP regions are defined by CAISO to aggregate demand response and other distributed sources and to define a basis for congestion revenue and capacity planning [16]. The SubLAP map of California can be found in [17]. With the analysis of SubLAPs, we showED the load shifting potential and benefits based on the local aggregation areas. The results for LMP savings were further analyzed for the hourly variation in a day.

Next, we analyzed the performance of different objective functions by comparing the results of the fixed-location model to solve the three problems in (1a), (1b), and (1c) and the results of the inter-location model to solve the three problems in (5a), (5b), and (5c). We analyzed the total LMP cost ((4a) and (10a)), the total MER ((4b) and (10b)), and the total RE ((4c) and (10c)) and recommended an objective to implement in more generally optimizing EV charging in electricity system operation.

Please note that the proposed optimization models are solved in Python, using an open-source modeling package called CVXPY [18].

## 3. Data

The main project data consist of actual vehicle telematics data from EVs, along with operational data for the electrical grid in California and the PG&E service territory. This allows us to estimate the economic and environmental benefits of load shifting in an ideal case, despite the strong assumptions of optimization, such as knowledge of vehicle arrivals, departures, and energy demand. Below, we describe the vehicle telematics data and the grid operational data, such as the LMP, the MER, and the RE, and we also briefly explain the pre-processing of the vehicle data.

### *3.1. Data Description*

We used telematics data from approximately 300 BMW electric and hybrid vehicles, whose drivers participated in this phase of the research project. The individual EV data describe the following anonymized types: the vehicle ID, the vehicle model, timestamps (for parking/charging events), the state of charge in the battery, the connection status of the vehicle to a charger, the vehicle location, and the odometer reading. The time period of data used for this analysis was from 10 November 2017 to 30 November 2017. BMW provided the information for battery capacity and the rated charging power for each vehicle model, as well as the anonymized home locations for each vehicle ID. The sample vehicles included BMW models i2, i8, and iPerformance, whose nominal rated charging powers ranged from 3.6 to 7.4 kW. The histogram for the actual charging power from the data is shown in Figure 3. The actual charging power deviates from the nominal charging power value; however, we used the nominal values for the rated charging power in (2) and (6).

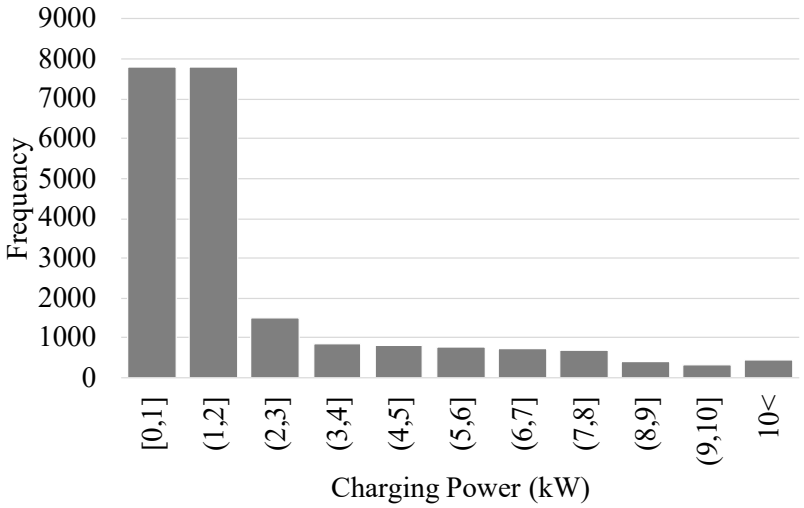


**Figure 3.** Histogram of actual charging power used by the electric and hybrid vehicle samples.

We obtained the day-ahead prices for the LMP data for the locations and times of parking sessions in the EV data. Each vehicle location given in latitude and longitude is matched to an LMP zone, the regional unit for which the LMP value is defined. The matching and gathering of LMP data were processed with an application programming interface tool by Kevala Analytics. Since LMP zones represent much larger geographic regions than the point values of latitude and longitude, the proposed models require much less precision for the location data. This may alleviate the privacy and accessibility issues with vehicle-location data for this type of analysis.

Due to data constraints, we obtained data of the MER and the RE ratio in different years to the driving data and the LMP data. We obtained the MER prediction values for every hour in 2019 from the ACC model. Data for the RE ratio for the total generated energy for every hour in 2018 were obtained from PG&E. The MER and the RE ratio do not include geographical information. Though it is possible that the MER and the RE ratio

values may change in trend, we tried our best to match the time periods of the driving data and LMP data by using the time period from 10 November 2019 to 30 November 2019 for MER and the time period from 10 November 2018 to 30 November 2018 for the RE ratio.

### *3.2. Data Processing*

The actual EV telematics data include anomalies, such as departure time before arrival time and negative values for the charging energy. These data, as well as data for vehicles that left California for any or all of the time period used, were excluded from the analysis. The percentage of the raw data that passed these criteria was 69.3%, i.e., the total vehicle-hours observed in the raw data and the processed data were 135,075 veh-hr and 93,576 veh-hr, respectively. For the fixed-location model, the desired energy at destination $k$, $E_{i,k}^{des}$, was the actual charging energy at destination $k$ in the data.

However, this actual charging energy was not used for the inter-location model. Instead, the energy consumption from the $k$-th destination to the next destination, $E_{i,k}^{c}$, was used. For the inter-location model, we processed the data to only contain the vehicles that have state-of-charge values at arrival always less than or equal to the state of charge values at the time of the previous departure. This is because if the state of charge is higher at arrival than at the previous departure, the charging energy demand is calculated as negative.

This anomaly can occur because some charging sessions are missing in the data. Not all parking instances are collected in the data, since the GPS tracking devices turn off when vehicles are on the move, and the vehicles may park inside some parking structures, where the GPS readings are unavailable. It is also possible that some plug-in hybrid EVs are charged during driving due to using gasoline and powering the vehicle generator. After this cleaning criteria, a data set with parking hours of 63,411 veh-hr was available for the inter-location model.

### *3.3. Data Flow*

Based on the proposed models and the real data of the EV telematics and the utility grid operation, we optimized the time and location of the EV charging sessions through the data flow shown in Figure 4. First, the EV telematics data were processed to meet the optimization model requirements as described in Section 3.2, based on the EV parameters, such as the rated charging power and battery capacities for each vehicle model. This processing outputs the clean data of parking and charging instances that can be used for the optimization with information on the time, the location, the battery state of charge, the original charging power and energy, and the transmission node connected to the parking location.

Second, the utility grid data on the LMP, the MER, and the RE were filtered according to the time and transmission nodes of the parking and charging instances. This helps reduce the memory required for computation because only a small subset of the available grid data can cover the times and locations present in the telematics data. Third, the parking and charging instances and the filtered grid data were used to solve the optimization problems proposed in (1a), (1b), and (1c) or in (5a), (5b), and (5c). Finally, the optimal results were outputted in terms of the optimal charging time, power, and energy. For the inter-location model, the charging location was also found. The final result also included the optimal grid performance for the aggregate EVs.

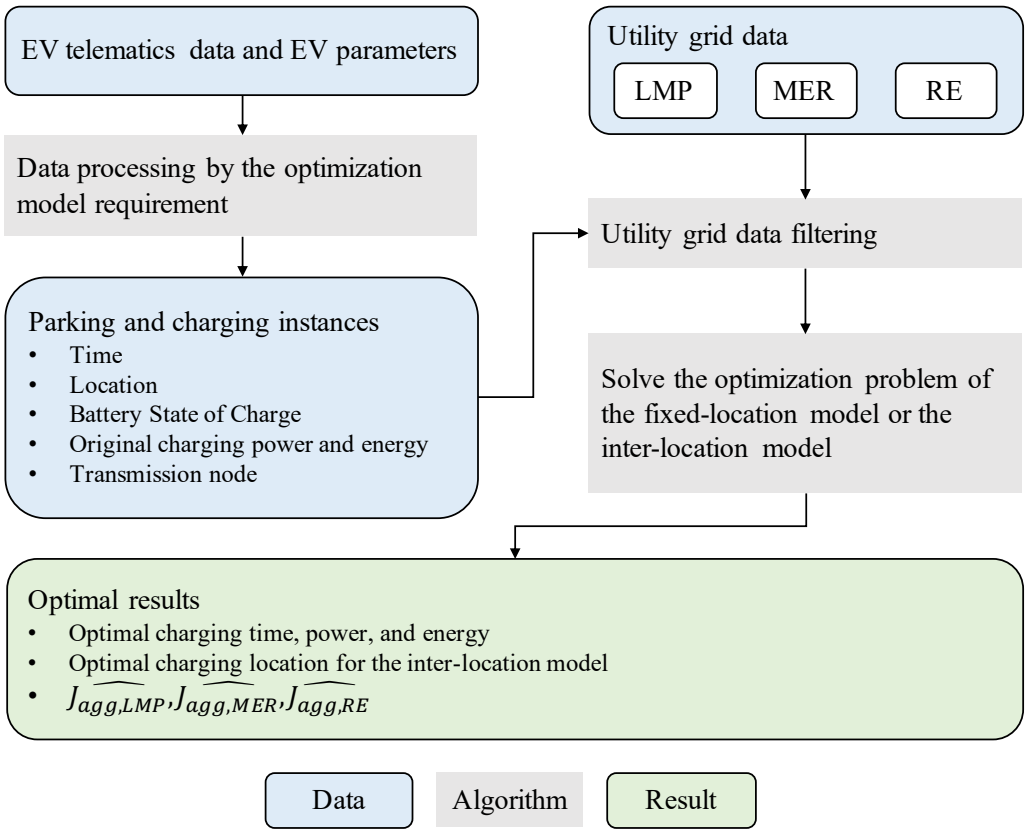


**Figure 4.** Data flow of the EV-charging optimization.

## 4. Results

In this section, we verify the fixed-location and inter-location models with sample trajectories of charging power of individual vehicles. We evaluated the two models based on the resulting locational marginal price cost, marginal emission rate, and renewable-energy ratio and showed that the inter-location model brings greater benefit to the electricity system operator than the fixed-location model. Additionally, we analyzed the optimization performances among three objective functions and made a recommendation for the energy system operator to use.

### *4.1. Fixed-Location Model of Charging Optimization*

We verified the optimization results of the fixed-location model, as shown in Figure 5, which shows the sample trajectories of charging powers of one vehicle in the actual data and the optimization result. The x-axis shows time; the left y-axis shows the charging power in kW; and the right y-axis shows the given LMP values in USD per MWh. The red dotted line plots the actual charging power in the data; the red continuous line plots the LMP-minimizing charging power; and the blue thick line plots the actual LMP values at the vehicle's current node during those hours $C_{\mathrm{LMP}}(t, \hat{x}_i(t))$. The figure shows one parking session in the optimized result, which lasted from 2 November 2017 12:00 a.m. to 11:00 p.m. In the actual data, the vehicle charged from midnight to 7:00 a.m. at 1.75 kW, though the LMP increased sharply in the morning around 5:00 a.m. The optimization result recommends charging at hours with low LMP values, this being early in the morning around 2:00 to 3:00 a.m. and around 11:00 a.m. to 5:00 p.m. The total charging energy in the optimal solution is the same as the actual charging schedule.

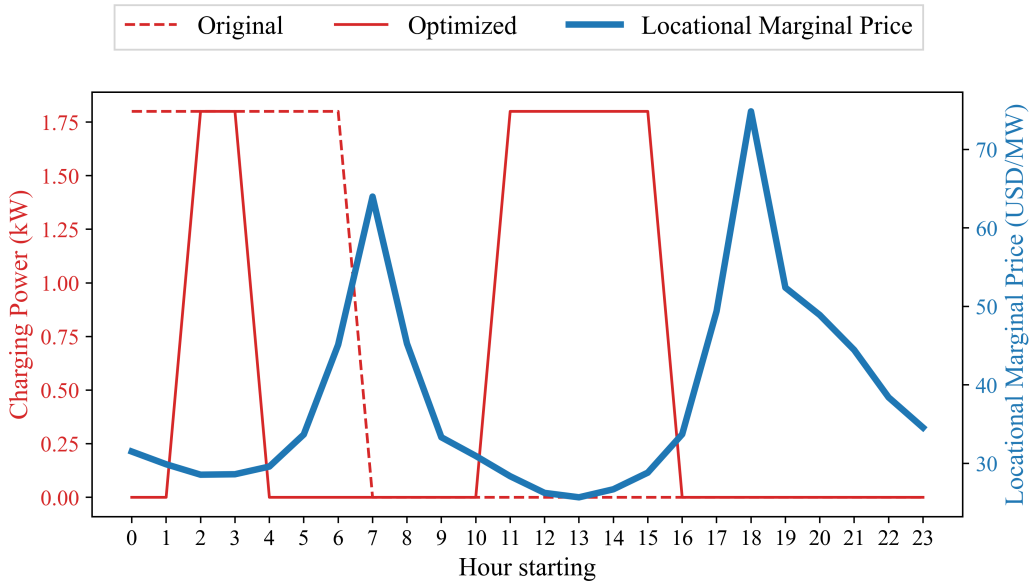


**Figure 5.** Sample trajectories of charging powers in the original data and the fixed-location model solution.

Table 1 presents the statistics of fixed-location results with LMP minimization, in terms of the total, home locations, and "away" locations. The statistics on total parking hours and total charging hours are the same in the original data and optimal results, as only the charging hours within each parking session are altered. Note that, on average, vehicles charge only 8.7% of the time in a day (15,383 veh-hr divided by 245 veh·24 h/day·30 days). Only 27.6% of the parking hours was used for charging (15,383 veh-hr divided by 55,819 veh-hr). This shows that there is ample flexibility for the EV drivers to choose the charging schedule; however, the vehicles mostly charge outside the optimal hours. The optimal charging schedule is different from the actual data by 12,374 veh-hr, which constitutes 80.4% of the total charging hours of the vehicles.

**Table 1.** Fixed-location result with LMP minimization.

| Item | Total | Home | Away |
|---|---|---|---|
| EV Sample Size (veh) | 245 | 196 | 138 |
| Total parking hours (veh-hr) | 93,576 | 72,170 | 21,406 |
| Total parking hours with charging events (veh-hr) | 55,819 | 48,099 | 7720 |
| Total charging hours (veh-hr) | 15,383 | 12,867 | 2516 |
| Total hours with a change in charging status due to optimization (veh-hr) | 12,374 | 10,608 | 1766 |
| Total change in LMP cost (USD, optimal—actual cost) for 30 days of sample | −236.8 | −205.8 | −31.1 |
| Average change in LMP cost * (USD/veh-hr) | −0.0025 | −0.0029 | −0.0015 |

* The denominator is the total parking hours—for example, 93,576 veh-hr for the total.

By significantly adjusting the charging hours, the LMP cost was reduced by USD 236.8 dollars for the fleet over a month. This is a significant savings, considering the relatively small level of the LMP cost (generally less than USD 100 per MW) and the small fleet size (245 vehicles in this case). This monthly savings can scale up directly if the number of participating EVs grows, where there are already more than 1000 times this many EVs in California with 256,000 registered in 2018 [19]. The LMP saving can also be calculated as USD 0.0025/veh/hr on average; in other words, there was an average gain of

USD 0.0025 in LMP savings for each hour that one vehicle staid in the system (or USD 0.06 for each day of one vehicle).

Analyzing the results in home and away locations separately, we see that the majority of the LMP cost reduction occurs at home, contributing to around 86.9% of the savings. One reason for this is because the vehicles park and charge more at home than away, so more adjustments are made to the charging schedule at home. Another reason is because the LMP peaks in the morning and the afternoon when people are primarily at home, so rescheduling charging powers at home brings benefits at a greater margin than at other locations.

### *4.2. Inter-Location Model of Charging Optimization*

We verified the optimization result of the inter-location model with Figure 6, which shows the actual and optimal charging power levels and LMP values for two consecutive parking events of one EV. The vehicle parked from 7:00 p.m. to 6:00 a.m. in the first parking session as shown in Figure 6a, drove for two hours, and parked from 8:00 a.m. to 4:00 p.m. in the second parking session as shown in Figure 6b. The axes and legends are similar to Figure 5.

We see that the inter-location model can schedule charging across multiple parking locations and hours, potentially recommending charging at locations and hours for lower LMP values. As seen in the top graph, the vehicle originally charged from midnight to 3:00 a.m., when the LMP cost was low. However, the model recommends that the vehicle be charged only shortly to exploit the lowest LMP cost at 2:00 a.m. in the first parking location, shifting the rest of the charging demand to the second parking location from 11:00 a.m. to 2:00 p.m., where the LMP cost was even lower for a longer period of time. Note that the optimization model has a hard constraint to meet the driver mobility needs. The model also ensures that the vehicle's state of charge is above a minimum level, $E_{min,i}$, at all times.

Table 2 presents the statistics for the inter-location model results with LMP minimization. The results are presented for the total, home locations, away locations, and two SubLAP regions. First, in total, we see that we had a smaller sample size of data for the inter-location model than for the fixed-location due to the data processing explained in Section 3.2. This suggests that, in practice, inter-location optimization will be more challenging than fixed-location optimization because of the data requirements for sequential and multi-location data. Additionally, the optimal solution charges vehicles at a lower number of hours and charging sessions, and the average charging power increases, compared to the actual behavioral data. This is because the optimization attempts to exploit lower-cost LMP hours by using its maximal charging power and avoids higher-cost LMP hours by reserving from charging. Therefore, the optimization result tends to decrease the total charging hours with more frequent charging instances and a higher average charging power.

Similar to the fixed-location model, the results showed a significant need to reschedule the charging sessions for better operation of the grid. The charging status changed from "idle" to "charging" or vice versa by the amount of 12,944 veh-hr, which was even greater than the original charging duration of 10,456 veh-hr. With this impact, the average LMP cost can be reduced by USD 369.5 dollars in total for 224 vehicles in a month, or USD 0.0059 per veh-hr. On average, the inter-location model produced about 2.36 times more LMP savings than the fixed-location model. This is because the inter-location model gives more freedom to reschedule the charging sessions and explore lower-cost LMP periods. In this model, the vehicles are recommended to change the charging hours, as well as the charging locations.

The results were compared for the home and "away" locations in the third and fourth columns of Table 2. Since the drivers tend to park and charge longer at home, the total parking and charging hours were much larger at home than away, as well as the number of total charging events. However, the optimal solution reduced charging hours and charging sessions more significantly at home than away, possibly because the vehicles were located

away from home (such as workplaces), when the LMP values were low during the day. We observed that there was a larger LMP saving at home than "away," first because there are originally more charging loads at home but also because the charging load was removed from home and added to the "away" locations.

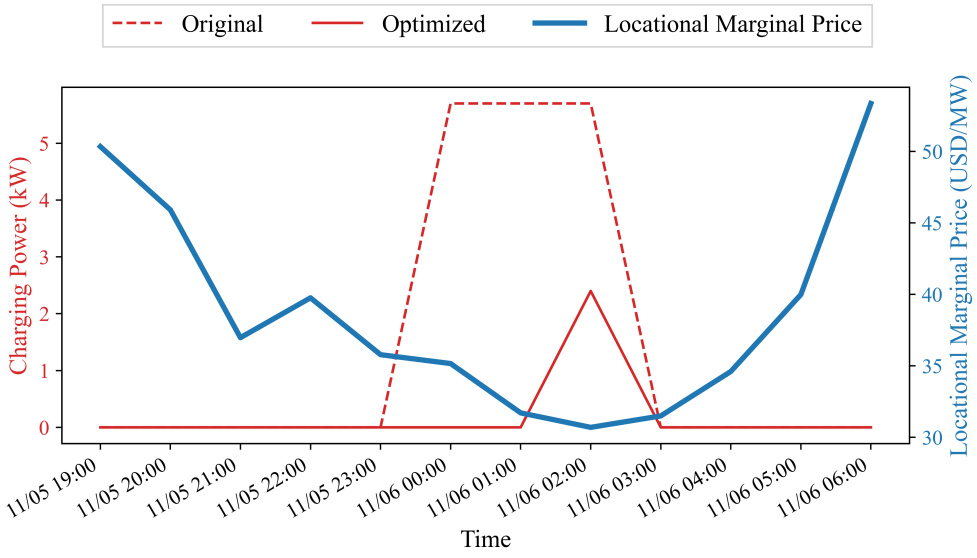


(**a**) Original Data

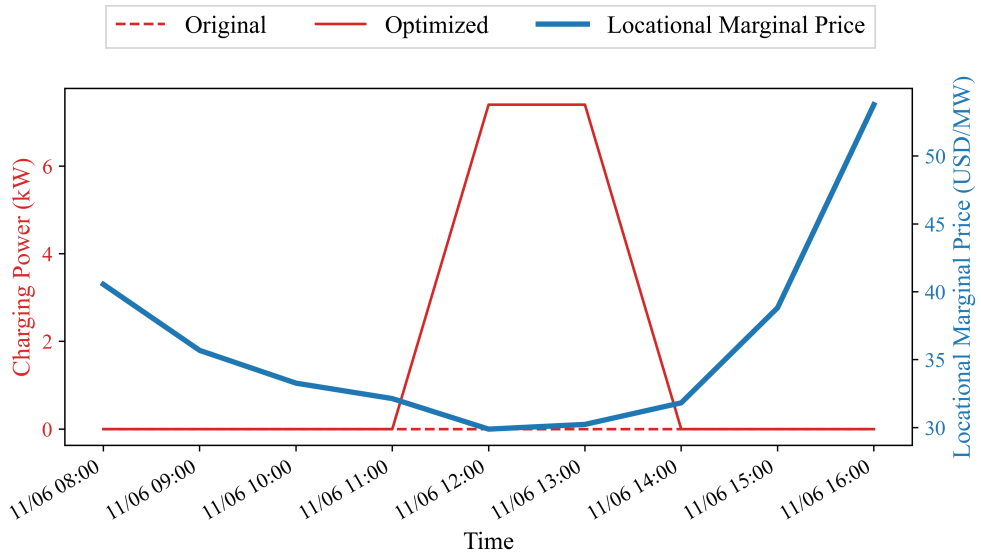


(**b**) Inter-Location Model

**Figure 6.** Sample trajectories of charging powers in the original data and the inter-location model solution.

Different SubLAPs also experience different results from optimization, as exemplified in the last two columns of Table 2. Among the 12 SubLAPs, PGP2 is a SubLAP around the San Francisco Peninsula area with the largest reduction in LMP cost and PGSI is a SubLAP around Sacramento, California, with the smallest reduction in LMP cost. Though the LMP values were not significantly different among the SubLAPs at the same hours, the total charging load can be very different among the SubLAPs. For instance, the actual charging energy was 7418.6 kWh in PGP2, which was much larger than the 285.9 kWh in PGSI, during the optimized time period. A larger LMP savings was expected to occur in regions with larger charging loads.

**Table 2.** Inter-location result with LMP minimization.

| Item | Total | Home | "Away" | PGP2 [2] | PGSI [3] |
|---|---|---|---|---|---|
| EV sample size (veh) | 224 | 173 | 211 | 109 | 4 |
| Total parking hours in actual data (veh-hr) | 63,411 | 48,522 | 14,889 | 21,429 | 577 |
| Total charging hours, actual data/optimized result (veh-hr) | 10,456/3812 | 8605/2644 | 1851/1168 | 3833/1208 | 42/44 |
| Total charging events, actual data/optimized result (events) | 2277/1818 | 1706/1151 | 571/667 | 752/584 | 12/17 |
| Average charging power, actual data/optimized result (kW) | 2.3/5.6 | 2.1/5.6 | 3.4/5.7 | 1.9/5.5 | 6.8/6.2 |
| Total hours with change in charging status due to optimization (veh-hr) | 12,944 | 10,309 | 2635 | 4621 | 86 |
| Total change in LMP cost (USD, optimal cost—actual cost) | −369.5 | −325.4 | −44.1 | −117.4 | −7.1 |
| Average change in LMP cost [1] (USD/veh-hr) | −0.0059 | −0.0067 | −0.0030 | −0.0055 | −0.0123 [4] |

[1] The denominator is the total parking hours in actual data; for instance, 63,411 veh-hr for the total. [2] Sublap example 1: Peninsula and Bay Area (PGP2). [3] Sublap example 2: Sacramento and Sierra (PGSI). [4] Though this result is presented for completeness, note that the sample size is only 4 vehicles, and this result does not carry statistical significance.

The hourly variation in LMP savings is depicted in Figure 7. The LMP cost in the optimal solution was larger than in the actual data from 9:00 a.m. to 2:00 p.m., because the charging load is was in these hours with low LMP values (California has high solar-energy generation and relatively low LMP costs in this period). The optimal solution suggests suppressing the charging of EVs when drivers are home from 3:00 p.m. to 8:00 a.m. the next day, and the LMP cost is greatly reduced in the afternoon. As a net outcome, the LMP saving from 3:00 p.m. to 8:00 a.m. was larger than the LMP increase from 9:00 a.m. to 2:00 p.m.

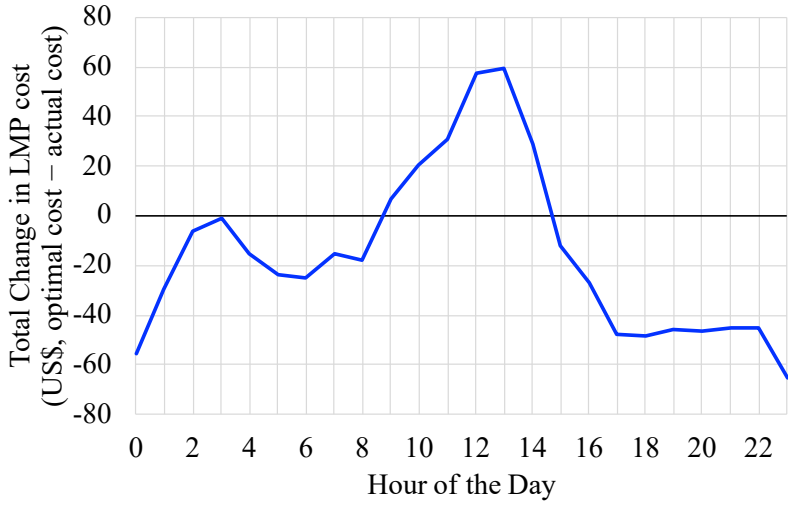


**Figure 7.** Hourly variation in total change in the LMP cost.

### *4.3. Optimization with Multiple Objectives*

We present a comprehensive analysis of the proposed models and objective functions to reschedule EV charging sessions and to improve electricity system operation. Figure 8 shows the results of the fixed-location and inter-location models with the three objective functions. (For the detailed results, refer to Table A1 in the Appendix A). The results are shown as a percentage difference relative to the actual data. For instance, the percentage

difference of the actual data from the LMP optimized result was calculated as (11), where $J_{\text{actual, LMP}}$ is the actual total LMP cost in the data.

$$\Delta_{\text{LMP}} = \frac{\widehat{J_{\text{agg, LMP}}} - J_{\text{actual, LMP}}}{J_{\text{actual, LMP}}} \cdot 100\% \tag{11}$$

Next, we extended the comparison of the fixed-location and inter-location models from the previous section to two additional objective functions, i.e., minimizing the MER and maximizing the RE. Figure 8 shows that the inter-location model reduced the MER and increased the RE to a greater extent compared with the fixed-location model. However, the inter-location model will be more challenging to implement in practice than the fixed-location model because the inter-location model makes more assumptions, such as the availability of sequential data for a vehicle's multiple destinations, accurate prediction of the vehicle's energy consumption, and successful relocation of charging sessions. Though the fixed-location model brings a smaller benefit than the inter-location model in theory, its easier implementation may result in better performance than the inter-location model in real-world settings.

We also compared the performance of the LMP, MER, and RE objective functions. For each optimization model, we observed that minimizing the LMP and the MER resulted in a similar performance in the LMP, the MER, and the RE. This is understandable from Figure 1, where the LMP and the MER have a very similar pattern over a sample day. Note that the RE value is relatively high at the start of the evening peak for LMP and MER. For instance, the RE ratio was around 0.3 to 0.6 from around 4:00 to 6:00 p.m. when the LMP and MER values were rapidly increasing. Therefore, maximizing the RE induces a substantial charging load during the peak hours of the LMP and the MER. Additionally, we see from Figure 8 that the RE-maximized solution increased the RE more than other solutions but did not largely improve the LMP or MER. This is understandable by observing Figure 9, where the optimal charging power to maximize the RE showed a different pattern to the charging powers to minimize the LMP or the MER. For instance, the RE-maximizing charging power was high at around 5 kW on average from 5:00 to 7:00 p.m., and the LMP-minimizing and MER-minimizing charging powers were much lower at below 3 kW. The start of the evening peak is a conflicting period because RE usage can be maximized with more charging but at a higher cost with rapidly increasing LMP and MER values. We observed that the fixed-location result for maximizing the RE results in a small increase in the LMP cost and a negligible increase in the MER.

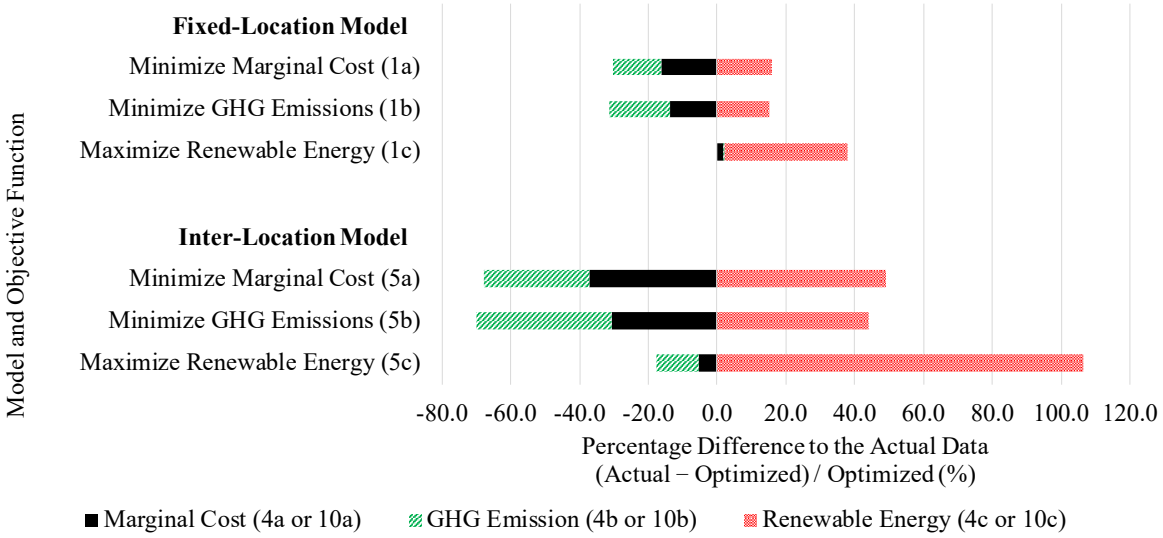


**Figure 8.** Comprehensive comparison of optimization models and objective functions on their economic and environmental performance (percentage difference explained via Equation (11)).

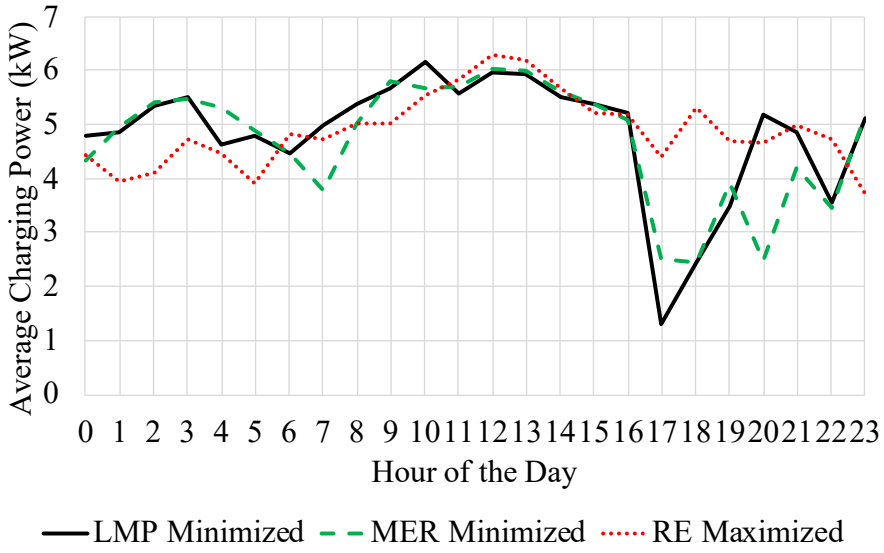


**Figure 9.** Optimal charging power of various objective functions (inter-location model).

### *4.4. Policy Implications*

Based on these results, we made a recommendation on the design of an EV-charging rescheduling program that improves electrical-grid performance. Currently the system operators for electricity generation, transmission, and distribution are subjected to various regulations and policies. For instance, California's Renewables Portfolio Standard (RPS) regulates the renewable energy procurement (in terms of delivered energy in watt-hours) to be at least 60% of the total energy by 2030 for "all electric load serving entities" [20]. Additionally, major electric power-generators in California must participate in California's Greenhouse Gas Cap-and-Trade Program to control their climate-related pollutants [21].

Among the various motivations for the grid-operators to optimize EV charging, we recommend programs for rescheduling EV charging focusing on grid congestion and cost (with respect to the LMP values) or to the emission level (with respect to the MER values) because they not only reduce marginal costs and emissions but also increase renewable usage. When renewable energy is maximized, it can induce more charging load at the start of peak hours with rapidly increasing demand, high grid congestion, and high marginal emission rates. Maximizing renewable energy in optimal EV charging can bring a substantial benefit to certain operators subjected to control their RE use; however, it can increase the burden on controlling grid congestion and emissions. Note that the renewable energy use can be increased with deployment of energy storage system, though it is more costly to upgrade grid infrastructure in this way than through controlled EV charging [7].

Assuming that the regional grid operation stays unaffected by the EV charging demand and rescheduling, we estimated the maximum improvements for the grid operation for about 250 EVs in Tables 1 and 2. As EV charging operation solutions scale much higher in the future, however, relative to the goal of California in deploying 5 million zero-emission vehicles by 2030 [22], the optimal EV charging can bring more benefits to the grid, but the large demand of charging will clearly affect grid operations, potentially in profound ways as highlighted by the large-scale simulation studies cited above. Extending this work to use growing amounts of real-world data to further evaluations of mass-scale EV charging optimization for improving the grid performance is the subject of future work.

In addition, we note that the current time-of-use (TOU) rate for EVs provided by PG&E for residential customers is not perfectly aligned with various goals of grid operation, such as reducing cost, reducing emissions, and increasing the use of renewable energy. For instance, on the PG&E "EV-B" plan in April 2021 [23], the energy cost is most expensive during the peak period at USD 0.56 per kWh from 2:00 p.m. to 9:00 p.m. However, this period may overlap with some hours with relatively low marginal cost, low marginal

emissions, and high renewable energy around 2:00 p.m. to 4:00 p.m. (shown in Figure 1). Under some conditions, grid operators may thus want to vary particularly the start time and also potentially the end times of peak TOU pricing periods during certain seasons with the potential to more fully maximize the benefits of EV charge timing to grid operations.

## 5. Future Work

Potential future work on this topic is as follows. First, this analysis did not explore the impact of shifting EV charging loads for the residential and workplace utility customer bills. For instance, utility demand charges (peak usage charges applied to commercial customers) can be impacted for EV-charging facility operators when loads are shifted across time and space. It is possible that the peak power and demand charges would increase due to a higher peak power of charging facilities, making the facility operator worse off, while the energy system operator is made better off. A potential negative effect on the electrical grid customers must be evaluated and solved, possibly with adjustments to the TOU energy and power pricing from the utilities.

Second, the impact of optimal EV charging on the electrical grid from a mass-scale level of implementation was not analyzed here, though several other studies have done this with simulations of a large EV fleet projected in the future. Utility grid performance can be affected by shifting the charging loads of a large fleet of EVs, expected in the future where, for instance, California has a goal of achieving 5 million zero-emission vehicles by 2030 [22]. In future work, the sample of individual EVs can be increased to reflect larger EV populations in the future. The EV charging can be optimized, and the grid performance can be evaluated with electrical-grid-operation simulators such as PLEXOS at the transmission level and/or PyDSS at the distribution level, accounting for additional grid factors such as changes in generation dispatch and power-quality issues, related to the large amount of load that can then be shifted on a regional basis.

Third, the analysis estimates the upper bound on the benefits to the electrical grid, but the lower bound is also important to better understand and advertise an optimal EV charging program. In other work, we have analyzed cases with current constraints on away-from-home charging, but in the future we expect EV-charging availability in between the current levels and the ubiquitous availability of charging assumed here. Further, the various factors that influence the success rate of optimal EV charging can be analyzed, such as driver compliance with the optimal charging schedule, uncertainty in driver response to their future trip plans, uncertain energy consumption during trips (due to speed, hills/grades, etc.), uncertain availability of chargers due to driver queuing, the potential impact of "power split" multi-port chargers, and mechanical or point-of-sale system failures. In future work, these factors can be parameterized to help further estimate the lower bound of the benefits. Behavioral surveys and focus groups and analysis of pilot studies on smart charging [24] can be used to better understand driver behavior and motivations in accepting a proposed optimal EV-charge-scheduling program. Additional key behavioral factors include driver adherence to planned departure times, driver propensity to plug in even when charging is not necessarily needed, and the statistical likelihood of sudden unplanned trips where the vehicles are unexpectedly disconnected.

## 6. Conclusions

This research estimated the maximum potential gains to electrical-grid operators in shifting the time and location of charging a sample group of EVs. We filled a gap in the literature by proposing optimization models that schedule not only the time but also the location to charge the individual EVs among the locations that they visit. The models were applied to three objective functions, based on the easily measurable and immediately meaningful values to the grid operator, including the locational marginal price cost, the greenhouse-gas emission rate, and the renewable-energy ratio. This work overcame the limitations of simulating or aggregating the driving and charging of EVs commonly found in the literature by using real data on a sample of individual, household-based EVs.

Collaborating with an automobile company, a grid operator, and two grid-services and energy data-analytics companies, this research used the driving and charging data of real individual EVs and the electrical grid data in the San Francisco Bay Area in California.

The results of the analysis showed a greater value in optimizing both the time and the location of charging EVs (inter-location model) than optimizing only the time of charging EVs (fixed-location model). However, the fixed-location optimal charging will be easier to implement in practice due to a simpler data requirement and a higher success rate from less uncertainty in trip demand and charging-schedule compliance. From the realistic estimation of the maximum benefits from optimal EV charging, it is recommended that grid operators consider the use of objective functions to reduce operational costs or marginal emission rates. These objective functions reduce grid operational costs and greenhouse-gas emissions, and they also increase renewable-energy usage. We do not recommend the maximization of renewable energy as a primary objective function as it can induce a higher load at the start of the evening peak, where renewable-energy generation is still high but where the energy load is ramping up with high marginal operation costs and emission rates. For the future work, the impact of shifting the EV-charging loads can be evaluated in terms of the residential and workplace utility bills for customers and the electrical grid performance. In addition, the lower bound of the benefits to the electrical grid from the optimal EV charging can be estimated.

**Author Contributions:** Conceptualization, S.W. and T.E.L.; methodology, S.W.; software, S.W. and Z.F.; validation, S.W., Z.F., E.A.-I. and T.E.L.; formal analysis, S.W. and Z.F.; investigation, S.W. and Z.F.; resources, T.E.L.; data curation, S.W. and Z.F.; writing—original draft preparation, S.W.; writing—review and editing, S.W., Z.F., E.A.-I. and T.E.L.; visualization, S.W.; supervision, T.E.L.; project administration, T.E.L.; funding acquisition, T.E.L. All authors have read and agreed to the published version of the manuscript.

**Funding:** This research was funded by the California Energy Commission EPIC Grant 15-084, led by BMW North America LLC and Pacific Gas and Electric Company.

**Institutional Review Board Statement:** Not applicable.

**Informed Consent Statement:** Not Applicable.

**Acknowledgments:** Olivine Inc. and Kevala Analytics Inc. provided critical project execution and analysis support.

**Conflicts of Interest:** The authors declare no conflict of interest.

## Nomenclature

The following abbreviations are used in this manuscript:

| | |
|---|---|
| EV | Electric vehicle |
| LMP | Locational marginal price |
| MER | Marginal emission rate |
| RE | Renewable energy |
| $N_{EV}$ | Sample size of EVs |
| $K_i$ | Number of locations that vehicle $i$ visits over the optimization time horizon |
| $i$ | Vehicle index, $i \in [1, N_{EV}]$ |
| $k$ | Destination index, $k \in [1, K_i]$ |
| $E_{b,i}$ | Battery capacity in energy for vehicle $i$ in kWh |
| $T^a_{i,k}$ | Arrival time to the destination node $k$ for vehicle $i$ |
| $T^d_{i,k}$ | Departure time from the destination node $k$ for vehicle $i$ |
| $E^{des}_{i,k}$ | Desired charging energy at the destination node $k$ for vehicle $i$ in kWh |
| $E^c_{i,k}$ | Energy consumption for the trip departing from the destination node $k$ for vehicle $i$ in kWh |
| $E_{ini,i}$ | Initial energy level in the battery of vehicle $i$ in kWh |
| $E_{min,i}$ | Minimum level of energy required for vehicle $i$ in kWh |

| | |
|---|---|
| $E_{max}$ | Maximum level of energy required for vehicle $i$ in kWh |
| $E_f$ | Final condition on the energy level required for vehicle $i$ in kWh |
| $S_i(t)$ | Parking status of vehicle $i$ at time $t$, which equals 1 if parked and 0 otherwise |
| $\hat{x}_i(t)$ | The electrical grid node that the location of vehicle $i$ belongs to |
| $\Delta t$ | Discrete time interval in hours |
| $P_{r,i}$ | Rated charging power of vehicle $i$ in kW |
| $P_c(i,t)$ | Charging power for vehicle $i$ at time $t$ in kW |
| $C_{\text{LMP}}(t,x)$ | Locational marginal price at time $t$ and node $x$ in USD/kWh |
| $C_{\text{MER}}(t)$ | Marginal emission rate at time $t$ in tons of $CO_2E$/kWh |
| $C_{\text{RE}}(t)$ | Renewable-energy ratio at time $t$, unitless |
| $\widetilde{J_{\text{agg, LMP}}}$ | The total LMP cost from the LMP-minimizing solution for aggregate EVs |
| $\widetilde{J_{\text{agg, MER}}}$ | The total MER from the MER-minimizing solution for aggregate EVs |
| $\widetilde{J_{\text{agg, RE}}}$ | The total RE from the RE-maximizing solution for aggregate EVs |

## Appendix A

Table A1 presents the detailed results of the fixed-location and inter-location models that optimize three objective functions, corresponding to Figure 8. Note that in the table, the performance metrics are the total resulting LMP cost, MER, and RE delivered.

**Table A1.** Comprehensive comparison of optimization models and objective functions on their economic and environmental performance.

| Model | Optimization | Performance Metric | | |
|---|---|---|---|---|
| | | **Total LMP Cost (US Dollars)** | **Total MER (Tons of $CO_2E$/kWh·kWh) **** | **Total RE (kWh)** |
| Fixed Location | None (Actual Data) | 1,892,127.3 | 22,851.2 | 18,540.4 |
| | LMP Minimized | 1,583,195.0 (−16.3%) | 19,619.4 (−14.1%) | 21,458.7 (15.7%) |
| | RE Maximized | 1,928,675.7 (1.9%) | 22,931.8 (0.4%) | 25,156.9 (35.7%) |
| | MER Minimized | 1,633,163.7 (−13.7%) | 18,822.2 (−17.6%) | 21,354.1 (15.2%) |
| Inter-Location Model | None (Actual Data) | 1,211,738.6 | 14,492.2 | 11,987.8 |
| | LMP Minimized | 762,861.9 (−37.0%) | 10,051.2 (−30.6%) | 17,871.8 (49.1%) |
| | RE Maximized | 1,146,037.2 (−5.4%) | 12,728.3 (−12.2%) | 24,745.9 (106.4%) |
| | MER Minimized | 839,052.8 (−30.8%) | 8,781.6 (−39.4%) | 17,277.6 (44.1%) |

This result calculates the total values for optimizing the charging of approximately 250 EVs after a data-cleaning process. To find the results per vehicle-hour, divide the results by the total parking hours of EVs in the data, which is 93,576 veh-hr for the fixed-location results and 63,411 veh-hr for the inter-location results. ** The MER parameter $C_{\text{MER}}(t)$ is given as a rate in tons of $CO_2E$/kWh, which indicates how many tons of emission will be produced per kWh when an additional load is given to the system. We calculated the "total MER" as the MER value multiplied by the charging energy in kWh. The limitation of this approach is the underestimation of marginal emissions, as the MER value may increase as more load is given to the system.

## References

1. Requia, W.J.; Mohamed, M.; Higgins, C.D.; Arain, A.; Ferguson, M. How clean are electric vehicles? Evidence-based review of the effects of electric mobility on air pollutants, greenhouse gas emissions and human health. *Atmos. Environ.* **2018**, *185*, 64–77. [CrossRef]
2. Spitzer, M.; Schlund, J.; Apostolaki-Iosifidou, E.; Pruckner, M. Optimized Integration of Electric Vehicles in Low Voltage Distribution Grids. *Energies* **2019**, *12*, 4059. [CrossRef]
3. Rizvi, S.A.A.; Xin, A.; Masood, A.; Iqbal, S.; Jan, M.U.; Rehman, H. Electric Vehicles and their Impacts on Integration into Power Grid: A Review. In Proceedings of the 2018 2nd IEEE Conference on Energy Internet and Energy System Integration (EI2), Beijing, China, 20–22 October 2018. [CrossRef]
4. Zheng, Y.; Niu, S.; Shang, Y.; Shao, Z.; Jian, L. Integrating plug-in electric vehicles into power grids: A comprehensive review on power interaction mode, scheduling methodology and mathematical foundation. *Renew. Sustain. Energy Rev.* **2019**, *112*, 424–439. [CrossRef]

5. van Triel, F.; Lipman, T.E. Modeling the Future California Electricity Grid and Renewable Energy Integration with Electric Vehicles. *Energies* **2020**, *13*, 5277. [CrossRef]
6. Zivin, J.S.G.; Kotchen, M.J.; Mansur, E.T. Spatial and temporal heterogeneity of marginal emissions: Implications for electric cars and other electricity-shifting policies. *J. Econ. Behav. Organ.* **2014**, *107*, 248–268. [CrossRef]
7. Szinai, J.K.; Sheppard, C.J.; Abhyankar, N.; Gopal, A.R. Reduced grid operating costs and renewable energy curtailment with electric vehicle charge management. *Energy Policy* **2020**, *136*, 111051. [CrossRef]
8. Kara, E.C.; Macdonald, J.S.; Black, D.; Bérges, M.; Hug, G.; Kiliccote, S. Estimating the benefits of electric vehicle smart charging at non-residential locations: A data-driven approach. *Appl. Energy* **2015**, *155*, 515–525. [CrossRef]
9. Tarroja, B.; Eichman, J.D.; Zhang, L.; Brown, T.M.; Samuelsen, S. The effectiveness of plug-in hybrid electric vehicles and renewable power in support of holistic environmental goals: Part 1—Evaluation of aggregate energy and greenhouse gas performance. *J. Power Sources* **2014**, *257*, 461–470. [CrossRef]
10. Jian, L.; Zheng, Y.; Shao, Z. High efficient valley-filling strategy for centralized coordinated charging of large-scale electric vehicles. *Appl. Energy* **2017**, *186*, 46–55. [CrossRef]
11. Teng, F.; Aunedi, M.; Strbac, G. Benefits of flexibility from smart electrified transportation and heating in the future UK electricity system. *Appl. Energy* **2016**, *167*, 420–431. [CrossRef]
12. Forrest, K.E.; Tarroja, B.; Zhang, L.; Shaffer, B.; Samuelsen, S. Charging a renewable future: The impact of electric vehicle charging intelligence on energy storage requirements to meet renewable portfolio standards. *J. Power Sources* **2016**, *336*, 63–74. [CrossRef]
13. Hoehne, C.G.; Chester, M.V. Optimizing plug-in electric vehicle and vehicle-to-grid charge scheduling to minimize carbon emissions. *Energy* **2016**, *115*, 646–657. [CrossRef]
14. Apostolaki-Iosifidou, E.; Pruckner, M.; Woo, S.; Lipman, T. Electric Vehicle Charge Management for Lowering Costs and Environmental Impact. In Proceedings of the 2020 IEEE Conference on Technologies for Sustainability (SusTech), Santa Ana, CA, USA, 23–25 April 2020. [CrossRef]
15. Singh, K.; Padhy, N.P.; Sharma, J. Influence of Price Responsive Demand Shifting Bidding on Congestion and LMP in Pool-Based Day-Ahead Electricity Markets. *IEEE Trans. Power Syst.* **2011**, *26*, 886–896. [CrossRef]
16. Alstone, P.; Potter, J.; Piette, M.A.; Schwartz, P.; Berger, M.A.; Dunn, L.N.; Smith, S.J.; Sohn, M.D.; Aghajanzadeh, A.; Stensson, S.; et al. *Demand Response Potential for California SubLAPs and Local Capacity Planning Areas: An Addendum to the 2025 California Demand Response Potential Study—Phase 2*; Technical Report; Lawrence Berkeley National Laboratory: Berkeley, CA, USA, 2017.
17. California ISO SubLAPs. Available online: https://www.pge.com/pge_global/common/pdfs/save-energy-money/energy-management-programs/demand-response-programs/2018-demand-response/2018-demand-response-auction-mechanism/PGE-Sub-Lap-Map-201703.pdf (accessed on 16 September 2019).
18. Diamond, S.; Boyd, S. CVXPY: A Python-embedded modeling language for convex optimization. *J. Mach. Learn. Res.* **2016**, *17*, 1–5.
19. Department of Energy: Alternative Fuels Data Center. Maps and Data-Electric Vehicle Registrations by State. Available online: https://afdc.energy.gov/data/10962 (accessed on 13 April 2021).
20. California Public Utilities Commission: RPS Program Overview. Available online: https://www.cpuc.ca.gov/rps_overview/ (accessed on 13 April 2021).
21. California Public Utilities Commission: Greenhouse Gas Cap-and-Trade Program. Available online: https://www.cpuc.ca.gov/general.aspx?id=5932 (accessed on 13 April 2021).
22. California Public Utilities Commission: Zero-Emission Vehicles. Available online: https://www.cpuc.ca.gov/zev/ (accessed on 13 April 2021).
23. Pacific Gas and Electric Company. Electric Schedule EV Residential Time-of-Use Service for Plug-in Electric Vehicle Customers. Available online: https://www.pge.com/tariffs/assets/pdf/tariffbook/ELEC_SCHEDS_EV%20(Sch).pdf (accessed on 15 April 2021).
24. Zeng, T.; Bae, S.; Travacca, B.; Moura, S. Inducing Human Behavior to Maximize Operation Performance at PEV Charging Station. *IEEE Trans. Smart Grid* **2021**, *12*, 3353–3363. [CrossRef]